Proceedings of ASME Turbo Expo 2011
GT2011
June 6-10, 2011, Vancouver, British Columbia, Canada

GT2011-46022

FUEL-FORCED FLAME RESPONSE OF A LEAN-PREMIXED COMBUSTOR

Poravee Orawannukul, Jong Guen Lee, Bryan D Quay and Domenic A Santavicca
Center for Advanced Power Generation
Department of Mechanical and Nuclear Engineering
The Pennsylvania State University
University Park, PA, USA

ABSTRACT

The response of a swirl-stabilized flame to equivalence ratio fluctuations is experimentally investigated in a single-nozzle lean premixed combustor. Equivalence ratio fluctuations are produced using a siren device to modulate the flow rate of fuel to the injector, while the air flow rate is kept constant. The magnitude and phase of the equivalence ratio fluctuations are measured near the exit of the nozzle using an infrared absorption technique. The flame response is characterized by the fluctuation in the flame's overall rate of heat release, which is determined from the total CH* chemiluminescence emission from the flame. The relationship between total CH* chemiluminescence intensity and the flame's overall rate of heat release is determined from a separate calibration experiment which accounts for the nonlinear relationship between chemiluminescence intensity and equivalence ratio. Measurements of the normalized equivalence ratio fluctuation and the normalized rate of heat release fluctuation are made over a range of modulation frequencies from 200 Hz to 440 Hz, which corresponds to Strouhal numbers from 0.4 to 2.8. These measurements are used to determine the fuel-forced flame transfer function which expresses the relationship between the equivalence ratio and rate of heat release fluctuations in terms of a gain and phase as a function of frequency. In addition, phase-synchronized CH* chemiluminescence images are captured to study the dynamics of the flame response over the modulation period. These measurements are made over a range of operating conditions and the results are analyzed to identify and better understand the mechanisms whereby equivalence ratio fluctuations result in fluctuations in the flame's overall rate of heat release. Such information is essential to guide the formulation and validation of analytical fuel-forced flame response models and hence to predict combustion dynamics in gas turbine combustors.

NOMENCLATURE

U:	mean velocity
T:	temperature
P_c:	combustor pressure
St:	Strouhal number
L_f:	flame length
R:	flame width
H:	flame transfer function
Q:	heat release rate
$\dot{m}_f$:	fuel mass flow rate
$\dot{m}_a$:	air mass flow rate
Δh_R:	heat of reaction
A:	flame area
S_L:	laminar flame speed
S_T:	turbulent flame speed
ρ:	density
u':	turbulent intensity
Ma:	Mach number
I_t:	transmitted intensity
I_o:	incident intensity
c:	absorbing concentration
l:	absorption path length

Greek symbol

ϕ:	equivalence ratio
β:	ratio of flame length to width
λ_ϕ:	convective wavelength
ω:	angular modulation frequency
ε:	the decadic molar absorption coefficient

Superscripts and Subscripts

‘:	amplitude in RMS of fluctuation
$_{mean}$:	mean value
$_T$:	total
$_{in}$:	inlet

INTRODUCTION

The generally accepted approach for meeting current and future NOx emissions regulations in land-based gas turbines is lean premixed combustion. Lean premixed gas turbine combustors, however, are more susceptible to combustion instabilities than are conventional diffusion flame combustors. The pressure oscillations associated with combustion dynamics can result in significant mechanical damages; therefore it is important to avoid their occurrence. Combustion instability is associated with the inherent coupling between system acoustics and unsteady heat release, and the amplification of this process due to feedback through one or more instability driving mechanisms. This is illustrated schematically in Figure 1, which also shows that the feedback can occur through velocity fluctuations and/or equivalence ratio fluctuations. Combustion instabilities are often referred to as self-excited instabilities.

The process whereby heat release fluctuations produce acoustic pressure fluctuations is well understood, however, the velocity fluctuation and equivalence ratio fluctuation mechanisms which provide the feedback needed to amplify the instability are not. Since it is difficult to study these instability driving mechanisms during a self-excited instability, so-called forced response tests are used to gain an understanding of these processes. Forced response tests involve the use of external forcing to produce a known fluctuation of the velocity (V') or equivalence ratio (ϕ') at the exit of the nozzle and measuring the flame's response in terms of the fluctuation of the overall rate of heat release ($\dot{Q}'$).

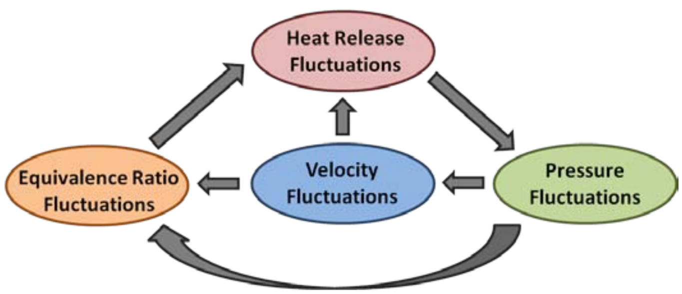

Figure 1: Self-Excited Oscillations in Partially Premixed Flames

Flame response measurement represents by flame transfer function. The flame transfer function has been defined as the flame response (heat release fluctuation) to time-varying combustor input parameters e.g. velocity and/or equivalence ratio perturbations with an assumption of negligible response to acoustic pressure fluctuations [1]. The flame transfer functions with inlet velocity fluctuations in premixed flames have been widely explored [2-6]. In both laminar and turbulent flames, three contributions that effect flame transfer functions are Strouhal number, St = $\omega L_f/U$, the ratio of flame length to width, $\beta = L_f/R$, and the flame shape, conical or "V" flames [2, 4, 6]. In general, the gain of flame transfer functions exhibits a low-pass filter behavior and its gain is amplified and dampened at certain frequencies. These amplification and damping of the gain indicate two or more competing mechanisms responsible for the flame response. For examples, the amplitude of flame transfer function is influenced by an interaction between flame and vortices generating in the outer jet shear layer [7]. Additionally, two competing mechanisms are reported: an axial acoustic perturbation which propagates with speed of sound and an azimuthal velocity perturbation which is convected at flow velocity was proposed [8].

In partially premixed flames, heat release fluctuation is consisted of two inlet perturbations: velocity and equivalence ratio fluctuations [1, 9]:

$$\frac{Q'}{\bar{Q}} = H_v(\omega)\frac{V'}{\bar{V}} + H_\phi(\omega)\frac{\phi'}{\bar{\phi}} \qquad (1)$$

Where H (or FTF) is flame transfer function of one input and one output flame response. In order to understand the flame response in partially premixed flame. Flame transfer functions under equivalence ratio perturbations are in needed.

The role of equivalence ratio oscillations was introduced as a driving mechanism in combustion instability [10]. There are limited studies on equivalence ratio fluctuation especially the experimental result on flame transfer functions. Most of studies are in numerical and analytical [11-15]. For analytical study of laminar premixed flame [11], three contributions controlled heat release fluctuation under equivalence ratio fluctuation are heat of reaction, flame speed and flame area fluctuations as shown in Fig. 2 [11]. Flame area fluctuation was an indirect effect for flame speed fluctuation. These three contributions changed the gain of transfer function to being amplified or damped. Also, amplification and destruction are not only depending on the magnitude response but also phases between three contributions. Changes in laminar flame speed resulted in flame front movement of 1.5 mm when equivalence ratio fluctuation is at 10 Hz [16].

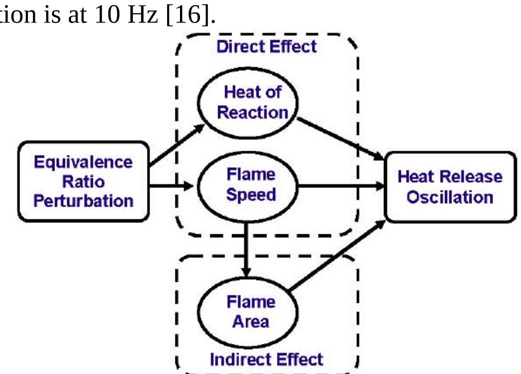

Figure 2: Mechanisms generating heat release oscillation caused by equivalence ratio perturbation in laminar premixed flames [11]

Saturation or non-linear behaviors in equivalence ratio fluctuations are studied [12-15, 17]. Analytically, heat release saturation mechanisms in this case are 1) flame-kinematic restoration and 2) nonlinear dependence of flame speed and heat of reaction on equivalence ratio [12]. Nonlinear behavior of an unconfined laminar "V" flame has been studied [14]. Phase-synchronized images showed wrinkling amplitude grew with distance from the injector and heat release saturation resulted from fuel pocket formations at the flame tip. Additionally, equivalence ratio fluctuations induced axial velocity fluctuations which interacted with the flame and modified the response at high levels of modulation. Similar result was found in LES flame response study at different modulation amplitudes that velocity fluctuation should be taking into account when forcing amplitudes are high [13]. However, the saturation of heat release fluctuation was not found and no large-scale vortices were observed even at 80% forcing amplitude. Nonlinear behaviors of turbulent flame were initiated at lower modulation amplitudes as forcing frequencies were higher [17]. Moreover, nonlinear behaviors were found when mean equivalence ratio was closer to lean blowoff. It was concluded that lean blowoff occurred when the normalized amplitude of equivalence ratio oscillation exceeded a threshold value which depended on mean equivalence ratio and modulation frequency.

As a result, flame transfer functions under equivalence ratio fluctuations should be explored experimentally in turbulent flames. The objectives of this paper are to experimentally measure and characterize the flame transfer function in ranges of inlet temperatures, velocities, equivalence ratio and pressures. Additionally, identify the underlying physics of flame's response to fuel flow rate fluctuations is very important to explain the cause and effect of the equivalence ratio fluctuation. As stated earlier, three disturbances dominate the heat release oscillations in laminar premixed flame as in Fig. 2. For turbulent premixed flames, the processes that involved are more complicated. A possible underlying physics schematic of heat release fluctuation due to equivalence ratio fluctuation in turbulent flame is shown in Fig. 3.

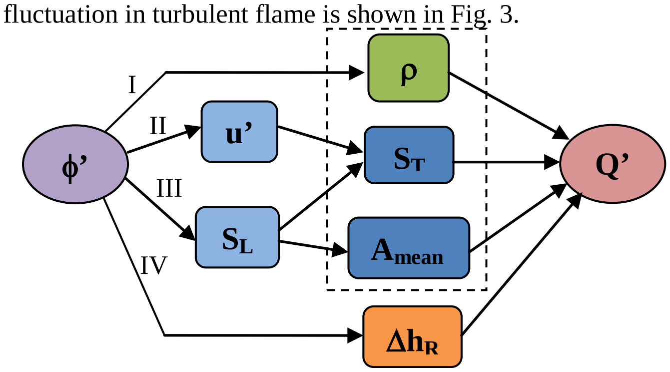

Figure 3: Possible mechanisms generating heat release oscillation caused by equivalence ratio perturbation in turbulent premixed flames

The derivation of Fig. 3 diagram is to begin with the definition of heat release rate:

$$\dot{Q} = \dot{m}_f \Delta h_R \qquad (2)$$

where the amount of fuel that being consume at the flame are the density of the fuel, turbulent flame speed and mean flame area (dash box in Fig. 3):

$$\dot{m}_f = \rho S_T A_{mean} \qquad (3)$$

The turbulent flame speed simply relates to the equivalence ratio via the turbulent intensity and laminar flame speed as shown in equation (4), (5) and (6). Moreover, laminar flame speed also affects the mean flame area.

$$S_T = S_L\left(1 + \frac{u'}{S_L}\right) \qquad (4)$$

$$S_L(\phi) = S_{L,o}(\phi)\left(\frac{T}{T_o}\right)^{\alpha(\phi)}\left(\frac{P}{P_o}\right)^{\beta(\phi)} \quad (5)$$

$$u' = 0.16 Re_h^{-1/8} \qquad (6)$$

Equation (5) is obtained from curve fit of the experimental laminar flame speed measurement where subscript "o" is the reference point at P_o=0.1 MPa and T_o=300 K [18]. Turbulent intensity is a function of hydraulic Reynolds number (equation 5) which in the system configuration is d_{outer}-d_{inner} where d is the diameter of the injector. The dependent on equivalence ratio of turbulent intensity is upon the density in the Reynolds number.

From Fig.3, equivalence ratio fluctuation affects the local mechanisms through four paths: I. density; II. turbulent intensity; III. laminar flame speed; and IV. heat of reaction. Each path may contribute to heat release fluctuation in different levels. Therefore, fluctuation in each path is calculated at equivalence ratio fluctuation normalized by mean of 4% RMS as an input. Heat of reaction equation is obtained [11] as:

$$\Delta h_R(\phi) = \frac{2.9125x10^6 \min(1,\phi)}{1+0.05825\phi} \qquad (6)$$

From the calculation, normalized density and turbulent intensity fluctuations by their mean are very small in order of 0.01 % RMS comparing with laminar flame speed and heat of reaction fluctuations which are in order of 10% and 1% RMS, respectively. This very small fluctuation in density is due to flow configuration is a subsonic flow which $Ma^2 << 1$, resulting in negligible density fluctuation [11]. As a result, path I and II in Fig.3 are negligible where path III and IV are important effects from equivalence ratio fluctuation.

EXPERIMENTAL SETUP

The experiment is performed in a lean-premixed, swirl-stabilized, single-nozzle gas turbine research combustor which is illustrated schematically in Fig. 4. The combustor consists of an inlet section, a siren device for fuel flow rate modulation, an injector, an optically-accessible quartz combustor and an exhaust section. The combustor is a cylindrical fused-sillica quartz with 150 mm diameter and 305 mm length. The natural combustion instability is found only at the longitudinal mode depending on the operating conditions. The rectangular combustor as shown in Fig. 4 is an outer part of the combustor which controls the pressure inside the combustor from 0 to 4 atm absolute pressure since RTV that seals between the cylindrical combustor and the injector holder can hold the pressure difference only 1-5 psig. The air is supplied by an air compressor and can be heated to 350°C using an 88 kW electric heater.

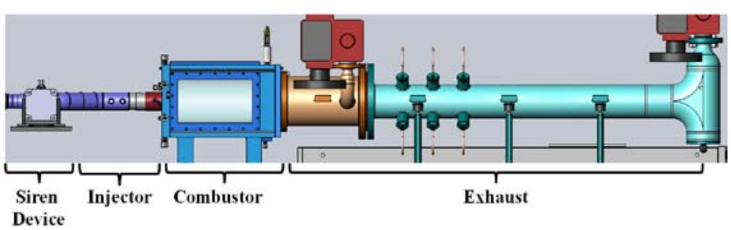

Figure 4 Optically accessible single-nozzle combustor.

The fuel is natural gas and is injected through holes in 45^o swirler vanes. The distance between the fuel injection locations to the combustor inlet is 101 mm. The siren has a capability to modulate the fuel flow rate at frequencies from 100 to 500 Hz. The modulation amplitude can be varied by changing the fraction of the fuel that bypasses the siren as shown in Fig. 5.

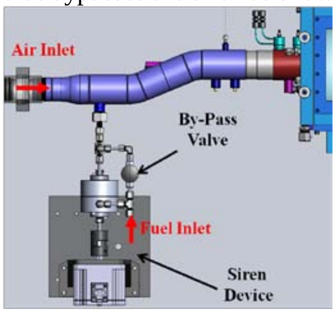

Figure 5: Siren device and flow schematic

MEASUREMENT TECHNIQUES

Measurements of the equivalence ratio fluctuation near the exit of the injector and of the fluctuation in the overall rate of heat release are needed to determine the flame transfer function. In addition, chemiluminescence imaging is used to characterize the flame structure at forced and unforced conditions; and dynamic pressure measurements are made in the injector in order to calculate the velocity fluctuation using the two-microphone technique [19].

Infrared Absorption

Equivalence ratio fluctuations near the exit of the nozzle are measured using an infrared absorption technique [20-21]. The absorption technique is a line-of-sight measurement which is described by the Beer-Lambert law:

$$\frac{I_t}{I_o} = e^{-\varepsilon c l} \quad (7)$$

where I_t and I_o are transmitted and incident intensities, respectively, ε is the decadic molar absorption coefficient, l is absorption path length and c is the concentration of the absorbing species. A He-Ne laser provides a coherent source of radiation at 3.39 um and thermoelectrically cooled indium-arsenide (InAs) detectors are used to measure the intensity of the infrared beam before and after passing through the injector, as illustrated in Fig. 6. Since the absorption technique is a line-of-sight measurement, the spatial fuel distribution must be uniform otherwise, measurement error will be unacceptable. In this experimental setup, the fuel distribution at the combustor inlet is spatially uniform within 3% RMS based on the acetone PLIF experiment.

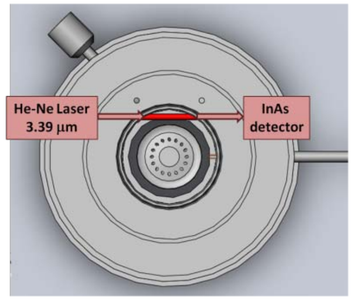

Figure 6: Schematic drawing of IR absorption measurement

A calibration curve, as shown in Fig. 7, relating the equivalence ratio to the ratio of the transmitted to incident intensity is produced. Since the absorption coefficient is a function of the gas pressure and temperature [20], calibration curves are needed for each operating condition.

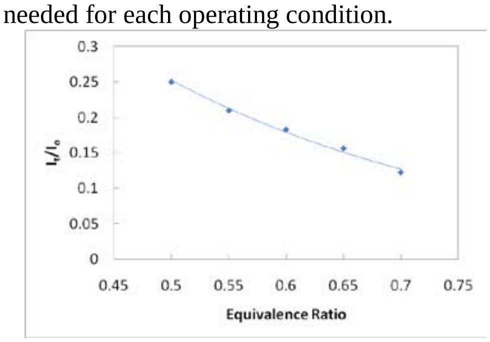

Figure 7: Calibration of equivalence ratio measurement at T_{in}=200^{o}C, U=25m/s, P_c=1atm

Total Chemiluminescence Intensity

The chemiluminescence intensity from the whole flame is measured using a photomultiplier tube with an interference filter which isolates the chemiluminescence emission from CH* (432 ± 5 nm), CO_2* (375 ± 5 nm) and OH* (307 ± 5 nm). The total chemiluminescence intensity from premixed flames with fixed equivalence ratio has been shown to increase linearly with the total rate of heat release, where the slope increases with increasing equivalence ratio [21-25]. This is an indicative of the nonlinear dependence of the chemiluminescence emission on equivalence ratio. Therefore, under the fuel-forced conditions of this study, the effects of changing equivalence ratio and rate of heat release on the total chemiluminescence emission must be accounted for [26]. If this is not done, the measured chemiluminescence intensity will overestimate the rate of heat release. To account for this, a calibration curve is produced which relates the total chemiluminescence intensity to the equivalence ratio for a fixed inlet temperature and velocity. An example of such a calibration curve is shown in Fig. 8, where the chemiluminescence intensity for all three chemiluminescence species is shown. This calibration curve is used to relate the measured fluctuation in the chemiluminescence intensity to the fluctuation in the equivalence ratio. Since the air flow rate is constant, the equivalence ratio fluctuation corresponds to the fluctuation in the rate of heat release.

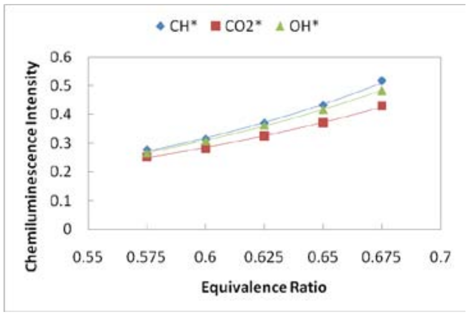

Figure 8: Chemiluminescence Calibration at T_{in}=200°C, U=25m/s, P_c=1atm

Chemiluminescence Flame Imaging

Images of the flame's chemiluminescence emission are used to determine the steady state and the forced flame structure. In their original form, the images are line-of-sight or projection images which do not reveal the interior structure of the flame. Using an Abel inversion, the two-dimensional structure of the flame is reconstructed from the line-of-sight image into a revolved image with radius weighted. The origin of the radius is from the centerline of the flame. The images are filtered (432 ± 5 nm) to isolated the CH* chemiluminescence emission and recorded using an intensified CCD camera (Princeton Instrument, PIMAX). The images are taken synchronized with the CH* chemiluminescence signal from PMT to study the flame behavior in a period of oscillation. Phase synchronized images are taken for forced flames where 100 individual images are taken every 15 phase-angle degrees with a 7.5 phase-angle degree gate width.

Dynamic Pressure

High frequency-response, water-cooled, piezoelectric pressure transducers are installed in the injector and combustor sections. Two transducers are located in the injector to measure velocity fluctuations using the Two-Microphone Method [27]. Velocity fluctuations are measured to ensure that these fluctuations are small and do not contribute to the measured fluctuation in the rate of heat release. The combustor pressure fluctuation is monitored by a pressure transducer mounted at the dump plane.

Experimental data (transmitted intensity for equivalence ratio fluctuation measurement, global chemiluminescence intensities and dynamic pressure transducers) are acquired by a data acquisition system at a sampling frequency of 8192 Hz. The corresponding frequency resolution of the measurements is 1 Hz. Spectral analysis of the signals is performed using a fast Fourier transform (FFT).

OPERATING CONDITIONS

Experiments are performed at inlet temperatures of 200°C and 275°C, at mean velocities (U) of 25, 30 and 35 m/s, at mean equivalence ratio ranging from 0.5-0.65 and at combustor pressure (P_c) of 1-2 atm (abs). Normalized equivalence ratio fluctuation amplitudes are up to 10% RMS depending on the modulation frequency. Flame transfer function measurements are at a fixed modulation amplitudes of 3.5-4% RMS. over a range modulation frequencies from 200 to 440 Hz in 20 Hz increments. The flame transfer function results are presented for both the fundamental and first harmonic frequencies, which corresponds to a range of Strouhal number of 0.4 to 2. The flame responses at the fundamental and harmonic frequencies are assumed to be independent. Phase-synchronized images are taken at one operating condition: T_{in}=275°C, U=30m/s, ϕ_{mean}=0.6, ϕ'_{RMS}/ϕ_{mean} = 4% and Strouhal number = 0.65 and 1.0.

RESULTS AND DICUSSIONS

Typical Flame Transfer Function

The flame transfer function of the equivalence ratio fluctuations is illustrated in equation (8) and the results are presented as plots of the gain and phase versus Strouhal number, St. Gain of the flame transfer function is the magnitude of the heat release and equivalence ratio fluctuations. Phase represents as the time required for the equivalence ratio perturbation to convect from the location of the infrared absorption measurement to the location in the flame where the equivalence ratio perturbation burns, convection time. Velocity fluctuation is negligible since the air flow rate is fixed and calculated coherences between the heat release fluctuation and velocity fluctuation are less than 0.9. The Strouhal number is a dimensionless parameter describing the oscillating flow mechanisms which separates the operating condition effect from the flame responses e.g. the mean thermal load [28]. It defines as ratio of the characteristic length of the flame to the flow perturbation which can be calculated as ratio of convection time to the oscillation period. In this experiment, the convection time is calculated from slope of the phase of the flame transfer function with modulation frequency. The characteristic length of the flow perturbation is given by the oscillation period (the reciprocal of perturbation frequency). The significant of the Strouhal number is to compare the flame to the perturbation characteristics. For instance, if the wavelength of the perturbation is greater than the flame length where the flame length is defined as the distance from the tip of the centerbody to the location of maximum chemiluminescence intensity in the chemiluminescence flame images, the Strouhal number is less than 1 and the flame is referred to as a compact flame. If the wavelength of perturbation is smaller than the flame length, the flame experiences different perturbation wavelength spatially acts a distributed source of heat release [29].

$$\boldsymbol{H_{\phi}(\omega)} = \left(\frac{\boldsymbol{Q\prime}}{\boldsymbol{\bar{Q}}}\right) / \left(\frac{\boldsymbol{\phi\prime}}{\boldsymbol{\bar{\phi}}}\right) \tag{8}$$

A typical flame transfer function result from this study is shown in Fig. 9. At low Strouhal number the gain is greater than 1 and there is a peak in the gain curve at a Strouhal number of approximately 0.7. As the Strouhal number is further increased, the gain decreases to values less than one and reaches a minimum at St ≈ 1.6. This is followed by a second, much smaller peak at St ≈ 1.9. Each data point in Fig. 9 corresponds to an average of 32 independent measurements and the error bars represent the measurement uncertainty with 95% confidence for a normal distribution. The characteristic of the gain will be discussed in flame imaging result.

Figure 9 also shows unwrap phase of the flame transfer function plotted versus the Strouhal number. Unwrapping the phase by subtracting 360^{o} is for continuity of the flame response. The phase is shown to increase linearly with Strouhal number. For the data shown in Fig. 9, the convection time is 2.4 ms. At this condition, the measured flame length is 7.5 cm, therefore, the mean convection speed is 29.4 m/s, as compared to the mean flow velocity in the injector of 30 m/s.

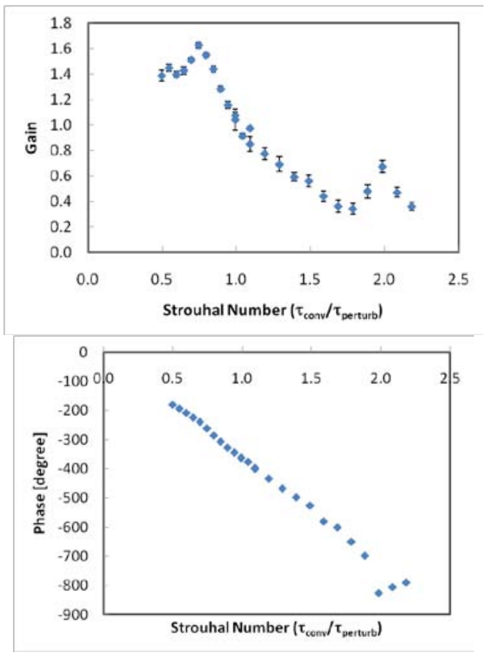

Figure 9: Gain (top) and Phase (bottom) of the Typical Flame Transfer Function at T_{in}=275^{o}C, U=30m/s, ϕ_{mean}=0.6, P_c=1atm

Effect of Inlet Temperature on the Flame Transfer Function

The effect of inlet temperature on the flame transfer function gain and phase is shown in Fig. 10. In this case, results are presented for inlet temperatures of 200°C and 275°C at constant velocity, equivalence ratio and pressure. Qualitatively the gain and phase results are very similar. There is a small shift in the Strouhal number at which the two peaks in the gain curve occur, shifting to lower Strouhal number with increasing temperature. There is also a small increase in the magnitude of the gain from St=0.5-1.0 with increasing temperature especially before the first peak. This is likely the result of the dependence of the laminar flame speed and heat of reaction on equivalence ratio for the conditions of this measurement according to Fig.3. The higher gain occurs at St <1 because the flame is a compact flame so the mean flame area fluctuation may have smaller effect of the flame responses. Mean flame area increases as laminar flame speed decreases. The phase results also show a small but discernable change in the slope with increasing temperature, which corresponds to a decrease in the convection time from 2.7 ms to 2.4 ms when the temperature is increased. Since the velocity is held constant, this indicates that the flame length shortens with increasing temperatures which can be attributed to an increase in the laminar flame speed.

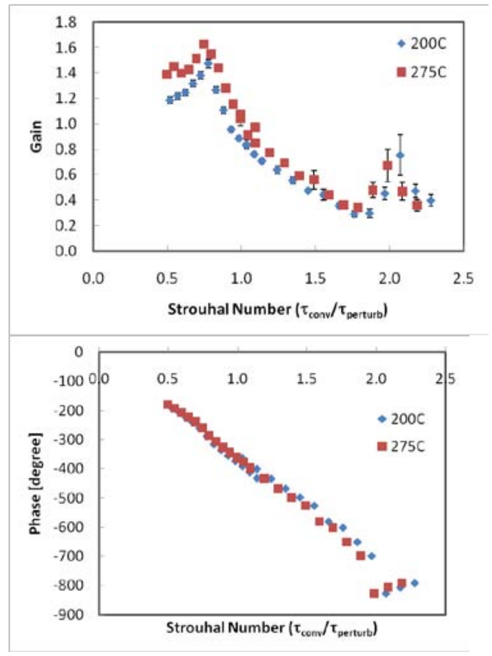

Figure 10: Gain (top) and Phase (bottom) of the Flame Transfer Functions at T_{in}=200^{o}C and 275^{o}C, U=30m/s, ϕ_{mean}=0.6, P_c=1atm

Effect of Mean Velocity on the Flame Transfer Functions

The effect of mean velocity on the flame transfer function is shown in Fig. 11. In this case the temperature (200°C) and equivalence ratio (0.6) are constant and results for mean velocities of 25 m/s, 30 m/s and 35 m/s are presented. Again the gain and phase results at different mean velocities are qualitatively similar. A possible explanation of similar gain magnitude in all cases is laminar flame speed and heat of reaction are fixed as the mean velocity changes so the flame responses are the same. The magnitude of the first peak in the gain curve, and the Strouhal number at which it occurs, show no measurable change with changing mean velocity. There is, however, a rather significant shift in the Strouhal number of the second peak, which shifts to lower Strouhal number as the mean velocity increases. There is also a change in the slope of the phase curves, corresponding to a change in the convection time from 3.1 ms to 2.7 ms to 2.3 ms as the velocity is increased which is clearly shown when plots with modulation frequency. The convection time is expected to decrease with increasing mean velocity and decreasing flame length. Since increasing velocity increases flame length and decreases convection time, this two effects take into account so plotting with the Strouhal number represents similar curves in all three different mean velocities.

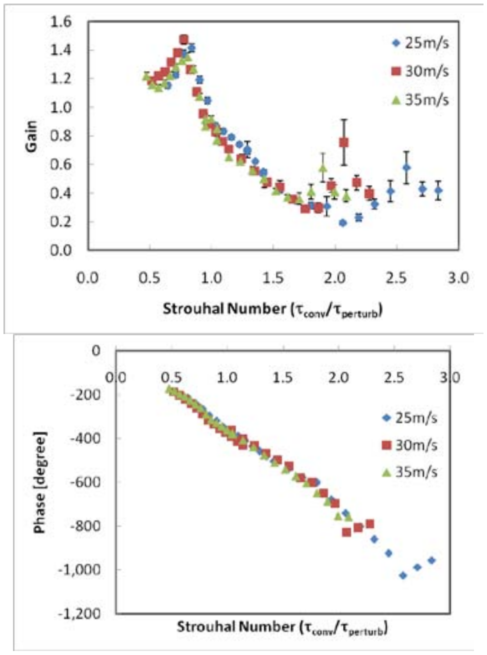

Figure 11: Gain (top) and Phase (bottom) of the Flame Transfer Functions at T_{in}=200^{o}C, U=25, 30 and 35 m/s, ϕ_{mean}=0.6, P_c=1atm

Effect of Mean Equivalence Ratio on the Flame Transfer Functions

The effect of equivalence ratio on the flame transfer function is shown in Fig. 12. In this case the temperature (275°C) and the velocity (30 m/s) are constant and results are presented for equivalence ratios of 0.55, 0.60 and 0.65. Again, the gain and phase results at different equivalence ratios are qualitatively similar. Both the magnitude of the first peak in the gain curve and the Strouhal number at which it occurs show no significant change with equivalence ratio. As was the case with the previous results (Figures 10 and 11), there is a small but discernable effect on the magnitude and Strouhal number of the second peak in the gain curve where both decrease with increasing equivalence ratio. The slope of the phase curves change when the equivalence ratio increases from 0.55 to 0.60, but not so when the equivalence ratio is increased to 0.65 in the plot with modulation frequency. Similarly, the convection time at an equivalence ratio of 0.55 is 2.8 ms, while the convection time is 2.4 ms second when the equivalence ratio is 0.60 and 0.65. This suggests that there is a change in the phenomenology of the flame's response to the equivalence ratio fluctuation that occurs near an equivalence ratio 0.55-0.60. From Fig.3, laminar flame speed and heat of reaction are increasing with increasing mean equivalence ratio. The percentage of increasing in heat of reaction is approximately the same ~8% using equation (6) as the mean equivalence ratio increases 0.05. However; the sensitivity of increasing from 0.55 to 0.6 and 0.6 to 0.65 is different in laminar flame speed. According to equation (5), laminar flame speed changes ~37% from 0.55 to 0.6 and ~27% from 0.6 to 0.65. The higher sensitivity of the laminar flame speed from 0.55 to 0.6 may explain why the gain of 0.55 and 0.6 is more different than other cases.

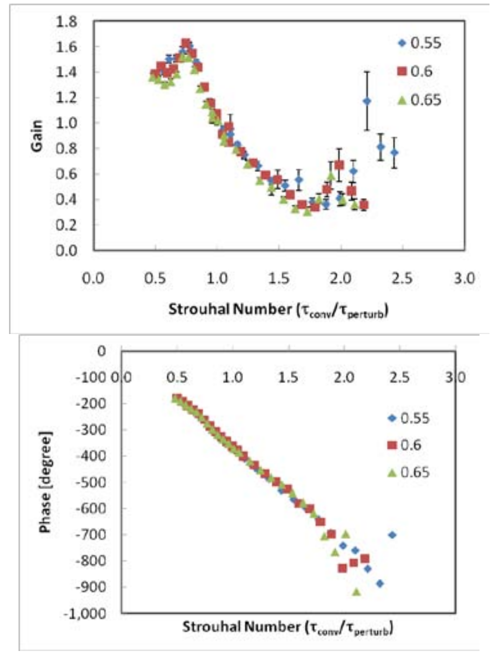

Figure 12: Gain (top) and Phase (bottom) of the Flame Transfer Functions at T_{in}=275^{o}C, U=30m/s, ϕ_{mean}=0.55, 0.60 and 0.65, P_c=1atm

Effect of Combustor Pressure on the Flame Transfer Functions

The effect of combustor pressure on the flame transfer function is shown in Fig. 13. In this case the temperature (275°C), the velocity (30 m/s) and the mean equivalence ratio are constant and results are presented for combustor pressure of 1 and 2 atm absolute. Qualitatively, the gain of 2 atm is higher than 1 atm before the first peak. The slope of the gain of 2 atm is steeper than 1 atm after the first peak. The second peak of 2 atm is not distinct and occurring at lower Strouhal number than 1 atm. The slope of the phase curves are different while plotting with modulation frequency. The convection time decreases from 2.4 ms to 2.0 ms as the pressure increases. The effect of pressure on the local mechanisms in Fig.3 is in both laminar flame speed and heat of reaction where increasing in pressure reducing the laminar flame speed but increasing the heat of reaction. An increase in heat of reaction may contribute larger effect on the flame response at St = 0.5-0.75 (before the first peak). After the first peak, the effect of mean flame area through the laminar flame speed may dominate the overall response since decreasing in laminar flame speed increases the mean flame area.

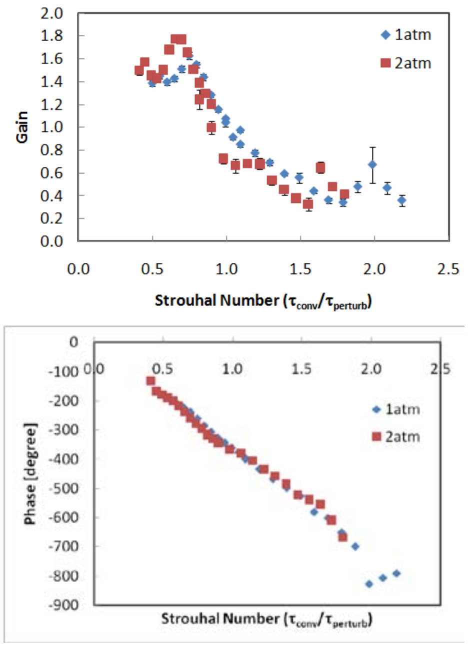

Figure 13: Gain (top) and Phase (bottom) of the Flame Transfer Functions at T_{in}=275°C, U=30m/s, ϕ_{mean}=0.60, P_c=1 and 2 atm

Comparing the Flame Transfer Functions of Equivalence Ratio Fluctuation with Velocity Fluctuation

All the flame transfer functions of all the operating conditions behave qualitatively as a low-pass filter as shown in Fig. 14, similar to velocity fluctuation studies [5-6]. However, the flame transfer functions of velocity fluctuation demonstrated a reduction in gain significantly at a certain frequency or Strouhal number. The flame transfer functions between velocity and equivalence ratio fluctuations are compared by evaluating a distinct point with the effect of mean equivalence ratio and mean velocity. The distinct point in velocity fluctuation would be the minimum gain and equivalence ratio fluctuation would be the 1st peak. In terms of the mean equivalence ratio effect on the flame transfer functions, the minimum gains are occurred at lower frequency as the mean equivalence ratio increases in velocity fluctuation [5]. This behavior is different from the gain from equivalence ratio fluctuation flame transfer function which is almost similar as the equivalence ratio is increasing. However, care must be taken in comparison since the operating mean equivalence ratios are different: ϕ_{mean}=0.55-0.65 in equivalence ratio fluctuation and ϕ_{mean}=0.65-0.80 in velocity fluctuation. For the mean velocity effect, the flame transfer functions exhibit similar behavior: the minimum gain or the 1st maximum occurs at a higher modulation frequency when the mean velocity increases. For the phase of the flame transfer functions, velocity fluctuation demonstrates an inflection point at a minimum gain frequency but this is not observed in equivalence ratio fluctuation case.

Generalized the Flame Transfer Functions

The flame transfer functions in equivalence ratio fluctuation can be scaled with Strouhal number from St = 0.4-2.8 as shown in Fig. 14 which strongly suggesting that the flame dynamics over different operating conditions could be generalized in terms of the relative length scale of the flame to convection length scale [30]. Moreover, scaling with Strouhal number may imply as the mechanisms that control the heat release fluctuation in equivalence ratio fluctuation are transported by convection. This statement will be supported by phase-synchronized images result in the next section. As St>1.5, the 2nd maximum occur at different Strouhal number may be implied that mechanisms at this range are different from prior range. Another dimensionless parameter could be applied to generalize the 2nd maximum. Two ranges of the Strouhal number, St=0.4-1.5 and St>1.5, may be separated by compact and non-compact flames. In addition to the flame transfer functions, the gain is amplified at low Strouhal number as stated earlier indicating there may be more than one mechanism influencing the flame response under equivalence ratio fluctuation which may be a combination of heat of reaction and laminar flame speed effects as illustrated in Fig.3.

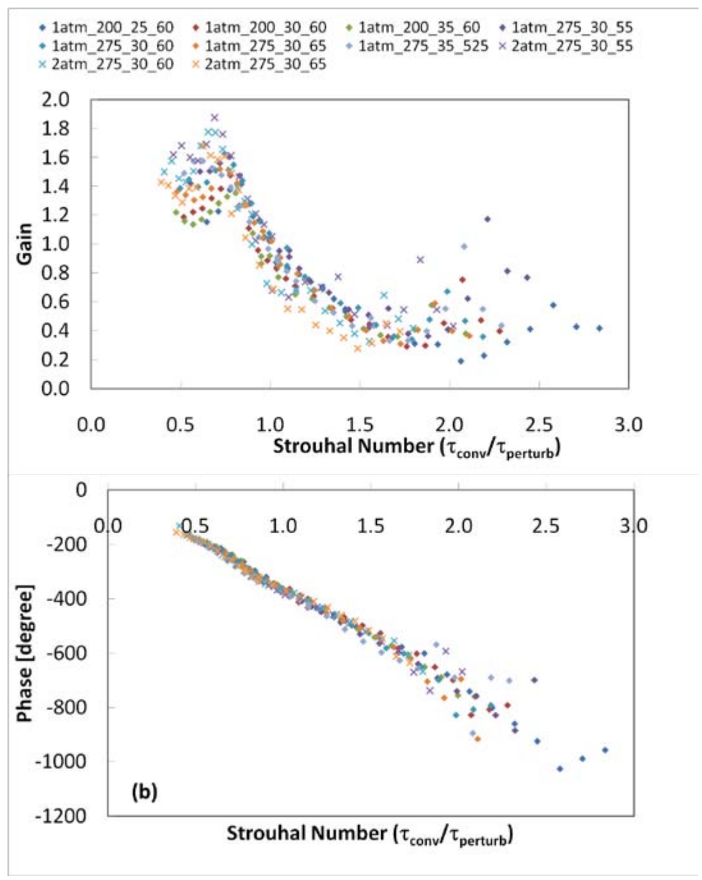

Figure 14: Gain (top) and Phase (bottom) of all the Flame Transfer Functions

Flame Imaging

In order to understanding the phenomenology of the flame's response to equivalence ratio fluctuation, measurements of the two-dimensional flame structure are made using CH* chemiluminescence imaging as shown in Fig.15. The flow direction is from left to right. The upper and lower halves of the flame are averaged because the flames are axisymmetric. The intensity of chemiluminescence is displayed in pseudocolor, with black being the lowest and white the highest intensity. Figure 15 shows the spatial and temporal evolution of the flame structure under forced conditions which is determined from phase-averaged deconvoluted chemiluminescence flame images. It presents a sequence of 24 phase-averaged flame images which are recorded in 15° phase angle increments. These images were taken at an inlet temperature of 275°C, a pressure of 1 atm, an inlet velocity of 30 m/s, a mean equivalence ratio of 0.6, a normalized RMS equivalence ratio fluctuation of 4%, and a Strouhal number of 0.65 and 1. As shown in Fig. 9, at Strouhal number of 0.65 the gain has a value of 1.4, which is very close to its maximum value, and this flame is a compact flame. Whereas; at Strouhal number of 1.0 the gain drops to 1.0, the flame is in the boundary between compact flame and non-compact flame regions.

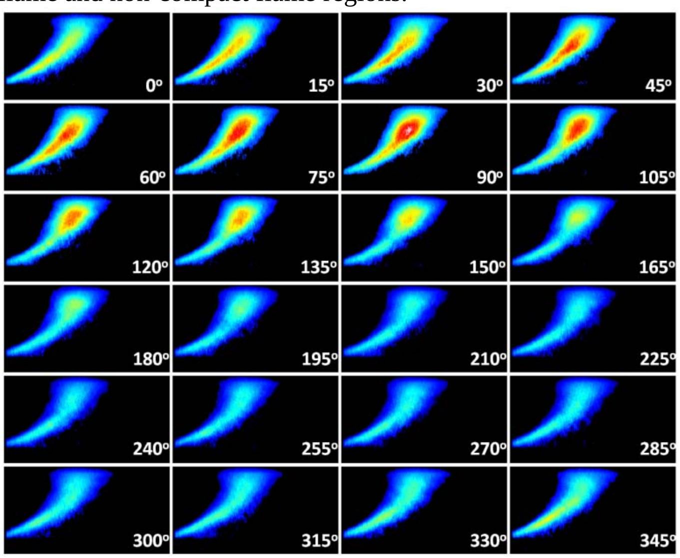

Figure 15: Phase-Synchronized-Deconvoluted Images of T_{in}=275°C, U=30m/s, ϕ_{mean}=0.6, ϕ'_{RMS}/ϕ_{mean} = 4% and Strouhal number = 0.65

Another way to present the images shown in Fig. 15 is in terms of fluctuation images. The fluctuation images are obtained by subtracting a time-averaged image of the forced flame, which is obtained by setting the exposure time on the camera to one forcing period, from the phase-averaged images. The fluctuation images corresponding to the phase-averaged images in Fig. 15 are shown in Fig. 16. The magnitude of the fluctuation is displayed in pseudocolor: red indicates that the fluctuation is positive or the local equivalence ratio is greater than the mean, light blue indicates that the fluctuation is zero or at the mean equivalence ratio, and blue indicates that the fluctuation is negative or the local equivalence ratio is lower than the mean. Fig.16 shows equivalence ratio fluctuation is convecting through the flame or flame experienced different equivalence ratio at each time e.g. at 0° phase flame is at equivalence ratio of 0.6 where at 90° flame is at 0.63. The dark lines surrounding the combined regions of positive and negative fluctuation represent the outer boundary of the flame. The black and magenta lines represent the boundary of the time-averaged and the phase-averaged images, respectively. Figure 16 shows that at this operating condition the overall shape of the flame changes very little during the forcing period. The fact that this is a compact flame is consistent with the observation that no more than one region of positive fluctuation and/or one region of negative fluctuation appear within the flame boundary at any given time. Similar results have been observed in both numerical and experimental studies of equivalence ratio fluctuation [13, 17].

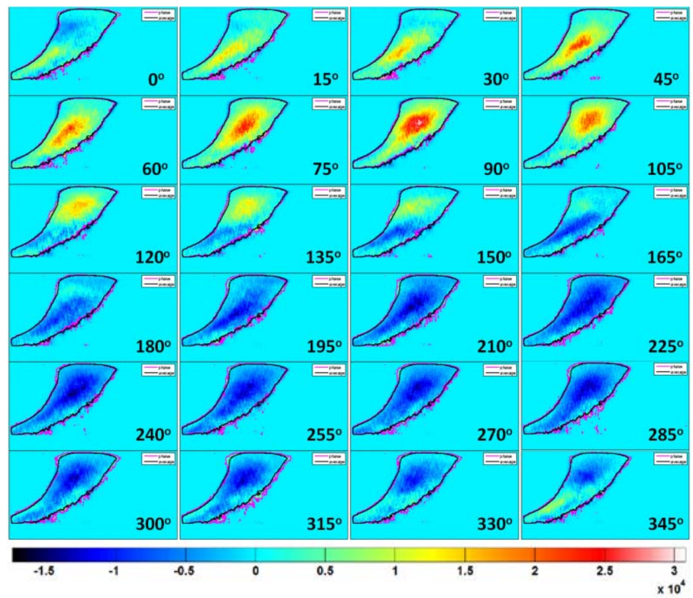

Figure 16: Phase-Synchronized-Deconvoluted-Fluctuation Images of T_{in}=275°C, U=30m/s, ϕ_{mean}=0.6, ϕ'_{RMS}/ϕ_{mean} = 4% and Strouhal number = 0.65

In the case Strouhal number of 1, the fluctuation images are shown in Fig. 17. The overall shape of the flame also changes very little over a period of oscillation similar to the Strouhal number of 0.65. Since the flame is in the boundary between compact and non-compact flame, there are evidences of two regions of positive and negative equivalence ratio within the flame boundary at any given time e.g. at 105°, 120°, 345°, etc but they are not distinct. The two regions are quantified by separating the flame at a given time into the positive and negative equivalence ratio as illustrated in Fig. 18. The intensity in the positive and negative equivalence ratio regions is added and plotted at a given time as shown in Fig. 19 and Fig. 20 for two Strouhal number cases. Figure 19 shows a compact flame has only one positive or negative region appeared at a given time as stated earlier. On the other hand, a non-compact flame has two regions in an image as shown in

Fig. 20. At a particular time where there are two regions, the flame response will be decreasing because of the dynamic of the fluctuating flame. A flame of lower equivalence ratio receives the support by the flame at higher equivalence ratio as a result; the overall heat release of this is smaller from a compact flame. The supporting phenomenon has been observed in a cylindrical flame [31]. From the cylindrical flame study, the flame under equivalence ratio fluctuation can be sustained even the local equivalence ratio exceeds the static lean blow off limit. Flame recovery phenomenon, or the supporting phenomenon, has an effect on the flame response when the Strouhal number is approximately 1 and higher. It is possible to combine the flame recovery effect with the local mechanisms proposed in Fig. 3. The flame recovery may occur because the mean flame area becomes more dominate on the flame response as it has opposite effect on the flame response with laminar flame speed and heat of reaction. In order to separate the local mechanisms, the mean flame area should be measurable by using the laser diagnostic technique which is left as a future work.

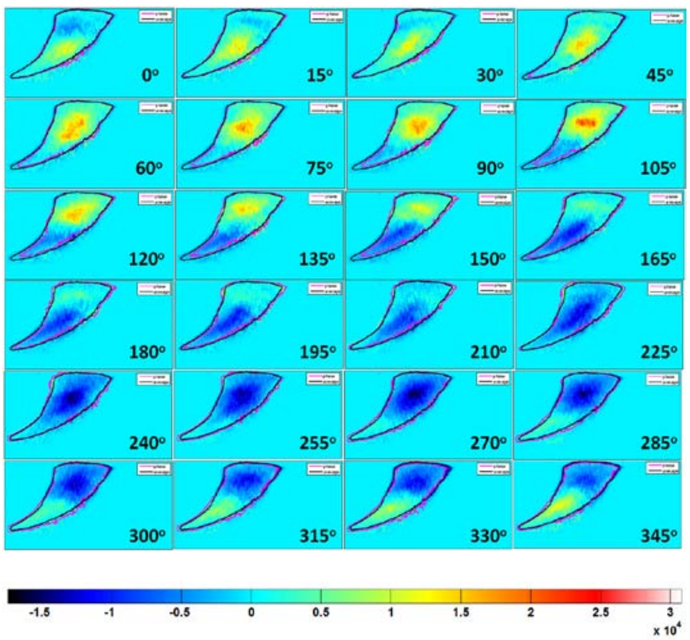

Figure 17: Phase-Synchronized-Deconvoluted-Fluctuation Images of T_{in}=275°C, U=30m/s, ϕ_{mean}=0.6, ϕ'_{RMS}/ϕ_{mean} = 4% and Strouhal number = 1.0

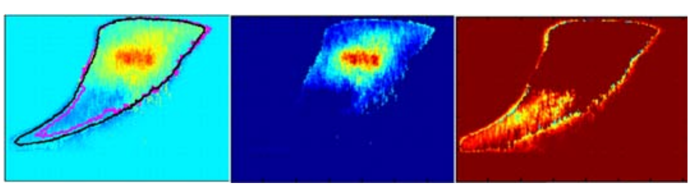

Figure 18: (left) Fluctuation Image, (center) positive equivalence ratio region (right) negative equivalence ratio region of T_{in}=275°C, U=30m/s, ϕ_{mean}=0.6, ϕ'_{RMS}/ϕ_{mean} = 4%, Strouhal number = 1.0 and phase angle = 105°

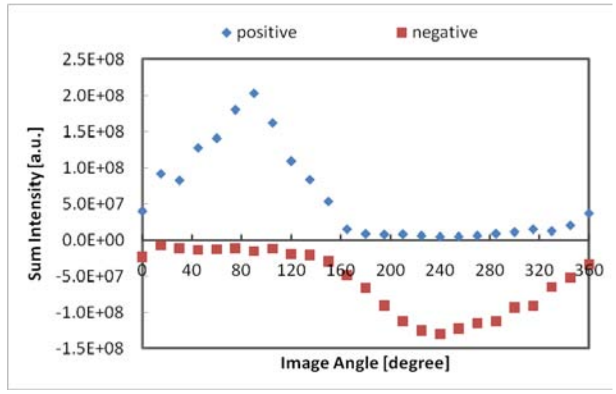

Figure 19: Intensity Summation of Positive and Negative Equivalence Ratio Regions of T_{in}=275°C, U=30m/s, ϕ_{mean}=0.6, ϕ'_{RMS}/ϕ_{mean} = 4% and Strouhal number = 0.65

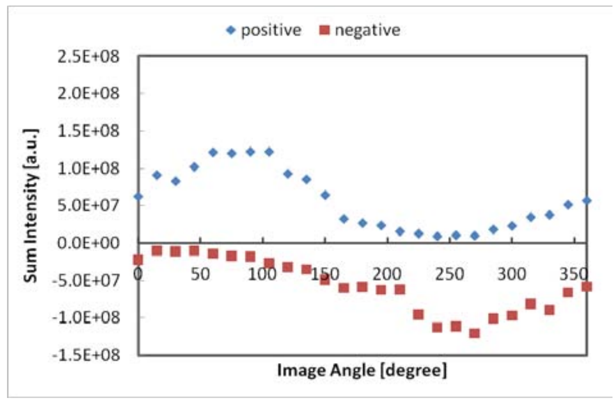

Figure 20: Intensity Summation of Positive and Negative Equivalence Ratio Regions of T_{in}=275°C, U=30m/s, ϕ_{mean}=0.6, ϕ'_{RMS}/ϕ_{mean} = 4% and Strouhal number = 1.0

CONCLUSION

An experimental study of flame response due to equivalence ratio fluctuation has been explored in ranges of mean velocities, mean equivalence ratio, inlet temperatures and combustor pressure. The gain of flame transfer function exhibits an overall low-pass filter behavior. Two peaks have found at a particular Strouhal number. There is a small increase in the magnitude of the gain at the first peak with increasing temperature but equally in changing the mean velocity. Decreasing the mean equivalence ratio to 0.55, phenomenology may be different than higher equivalence ratio (0.6 and 0.65) due to the flame speed sensitivity. Combustor pressure does increase the flame response at low Strouhal number but decrease at higher Strouhal number. Comparing the flame transfer functions with velocity fluctuation case, the flame transfer functions show similar trend in the mean velocity effect but different in the mean equivalence ratio effect. Phase-synchronized images illustrated a high intensity region convecting through the flame to downstream without modifying the flame brush. Flame response due to equivalence ratio fluctuation is suggested to be convective. The reduction in gain of the flame transfer function is possibly explained from the Strouhal number effect with the flame recovery phenomenon. The local mechanisms beyond heat release fluctuation causes by equivalence ratio are proposed. The main components are laminar flame speed and heat of reaction where turbulent flame speed and mean flame area fluctuations are the effects of the laminar flame speed. Identification of each mechanism will be performed in depth as a future work so as the studies in effect of pressure and fuel composition on flame transfer functions and the 2nd maximum characteristic.

REFERENCES

[1] Huber, A., and Polifke, W., "Impact of Fuel Supply Impedance on Combustion Instability of Gas Turbines," Proc. Proceedings of ASME Turbo Expo 2008: Power for Land, Sea and Air.

[2] Fleifil, M., Annaswamy, A. M., Ghoneim, Z. A., and Ghoniem, A. F., 1996, "Response of a Laminar Premixed Flame to Flow Oscillations: A Kinematic Model and Thermoacoustic Instability Results," Combustion and Flame, 106, pp. 487-510.

[3] Schuller, T., Durox, D., and Candel, S., 2003, "A Unified Model for the Prediction of Laminar Flame Transfer Functions: Comparisons Between Conical and V-Flame Dynamics," Combustion and Flame, 134, pp. 21-34.

[4] Lieuwen, T., and Bellows, B., "Nonlinear Kinematic Response of Premixed Flames to Harmonic Velocity Disturbances," Proc. Proceedings of the Combustion Institute, pp. 1725-1732.

[5] Brian Jones, J. G. L., Bryan D. Quay and Domenic A. Santavicca, 2011, "Flame Response Mechanisms due to Velocity Perturbations in a Lean Premixed Gas Turbine Combustor," Journal of Engineering for Gas Turbines and Power, 133.

[6] Kim, K. T., Lee, J. G., Lee, H. J., Quay, B. D., and Santavicca, D. A., 2010, "Characterization of Forced Flame Response of Swirl-Stabilized Turbulent Premixed Flames," Journal of Engineering for Gas Turbines and Power, 132.

[7] D. Durox, T. S. a. S. C., "Combustion Dynamics of Inverted Conical Flames," Proc. Proceedings of the Combustion Institute, pp. 1717-1724.

[8] P. Palies, D. D., T. Schuller and S. Candel, 2010, "The Combine Dynamics of Swirler and Turbulent Premixed Swirling Flames," Combustion and Flame, 157, pp. 1698-1717.

[9] Schuermans, B., Guethe, F., and Mohr, W., "Optical Transfer Function Measurements for Technically Premixed Flames," Proc. Proceedings of ASME Turbo Expo 2008: Power for Land, Sea and Air.

[10] Lieuwen, T., and Zinn, B. T., 1998, "The Role of Equivalence Ratio Oscillations in Driving Combustion Instabilities in Low NO_x Gas Turbines," Twenty-Seventh Symposium (International) on Combustion, The Combustion Institute, pp. 1809-1816.

[11] Cho, J. H., and Lieuwen, T., 2005, "Laminar Premixed Flame Response to Equivalence Ratio Oscillations," Combustion and Flame, 140, pp. 116-129.

[12] H., S., Shreekrishna, and Lieuwen, T., 2007, "Premixed Flame Response to Equivalence Ratio Perturbations," 43rd AIAA/ASME/SAE/ASEE Joint Propulsion Conference & ExhibitCincinnati, OH.

[13] Sengissen, A. X., Kampen, J. F. V., Huls, R. A., Stoffels, G. G. M., Kok, J. B. W., and Poinsot, T. J., 2007, "LES and Experimental Studies of Cold and Reacting Flow in a Swirled Partially Premixed Burner with and without Fuel Modulation," Combustion and Flame, 150, pp. 40-53.

[14] Birbaud, A. L., Ducruix, S., Durox, D., and Candel, S., 2008, "The Nonlinear Response of Inverted "V" Flames to Equivalence Ratio Nonuniformities," Combustion and Flame, 154, pp. 356-367.

[15] Sankaran, R., and Im, H. G., "Dynamic Flammability Limits of Methane/Air Premixed Flames with Mixture Composition Fluctuations," Proc. Proceedings of the Combustion Institute, pp. 77-84.

[16] Ax, H., Kutne, P., Meier, W., Konig, K., Maas, U., Class, A., and Aigner, M., 2009, "Low Pressure Premixed CH_4/Air Flames with Forced Periodic Mixture Fraction Oscillations: Experimental Approach," Applied Physics B: Lasers and Optics, 94, pp. 705-714.

[17] Kim, K. T., Lee, J. G., Quay, B. D., and Santavicca, D. A., "Experimental Investigation of the Nonllinear Response of Swirl-Stabilized Flames to Equivalence Ratio Oscillations," Proc. Proceedings of ASME Turbo Expo 2010: Power for Land, Sea and Air.

[18] Liao, S. Y., Jiang, D. M., and Cheng, Q., 2004, "Determination of laminar burning velocities for natural gas," Fuel, 83, pp. 1247-1250.

[19] Ross, A. F. S. a. D. F., 1976, "Experimental Determination of Acoustic Properties using a Two-Microphone Random-Excitation Technique," Journal of the Acoustical Society of America, 61(5), pp. 1362-1370.

[20] Lee, J. G., Kim, K., and Santavicca, D. A., "Measurement of Equivalence Ratio Fluctuation and Its Effect on Heat Release During Unstable Combustion," Proc. Proceedings of the Combustion Institute, pp. 415-421.

[21] Lee, J. G., and Santavicca, D. A., 2003, "Experimental Diagnostics for the Study of Combustion Instabilities in Lean Premixed Combustors," Journal of Propulsion and Power, 19(5), pp. 735-750.

[22] Samaniego, J. M., Egolfopoulos, F. N., and Bowman, C. T., 1995, "CO_2^* Chemiluminescence in Premixed Flames," Combustion Science and Technology, 109, pp. 183-203.

[23] Higgins, B., McQuay, M. Q., Lacas, F., Rolon, J. C., Darabiha, N., and Candel, S., 2001, "Systematic Measurements of OH Chemiluminescence for Fuel-Lean, High-Pressure, Premixed, Laminar Flames," Fuel, 80, pp. 67-74.

[24] Huber, L. C., Vandsburger, U., Saunders, W. R., and Khanna, V. K., "An Experimental Examination of the Relationship between Chemiluminescence Light Emissions and Heat-Release Rate Under Non-Adiabatic Conditions," RTO/AVT Symposium: Propulsion and Power System.

[25] Hardalupas, Y., and Orain, M., 2004, "Local Measurements of the Time-Dependent Heat Release Rate and Equivalence Ratio using Chemiluminescence Emission from a Flame," Combustion and Flame, 139, pp. 188-207

[26] Lauer, M., and Sattelmayer, T., 2010, "On the Adequacy of Chemiluminescence as a Measure for Heat Release in

Turbulent Flames with Mixture Gradients," Journal of Engineering for Gas Turbines and Power, 132.
[27] Seybert, A. F., and Ross, D. F., 1976, "Experimental Determination of Acoustic Properties using a Two-Microphone Random-Excitation Technique," Journal of the Acoustical Society of America, 61(5), pp. 1362-1370.
[28] Buchner, C. K. a. H., 2002, "Combustion Dynamics of Turbulent Swirling Flames," Combustion and Flame, 131, pp. 70-84.
[29] Lieuwen, J. H. C. a. T., 2005, "Larmina Premixed Flame Response to Equivalence Ratio Oscillations," Combustion and Flame, 140, pp. 116-129.
[30] Kim, D., Lee, J. G., Quay, B. D., and Santavicca, D., "Effect of flame structure on the flame transfer function in a premixed gas turbine combustor," Proc. Proceedings of FT2008 ASME Turbo Expo 2008: Power for Land, Sea and Air.
[31] Suenaga, Y., Kitano, M., and Takahashi, Y., 2010, "Propagation and Extinction of a Cylindrical Premixed Flame Undergoing Equivalence Ratio Fluctuation Near the Lean Limit," Journal of Thermal Science and Technology, 5(1), pp. 124-134.